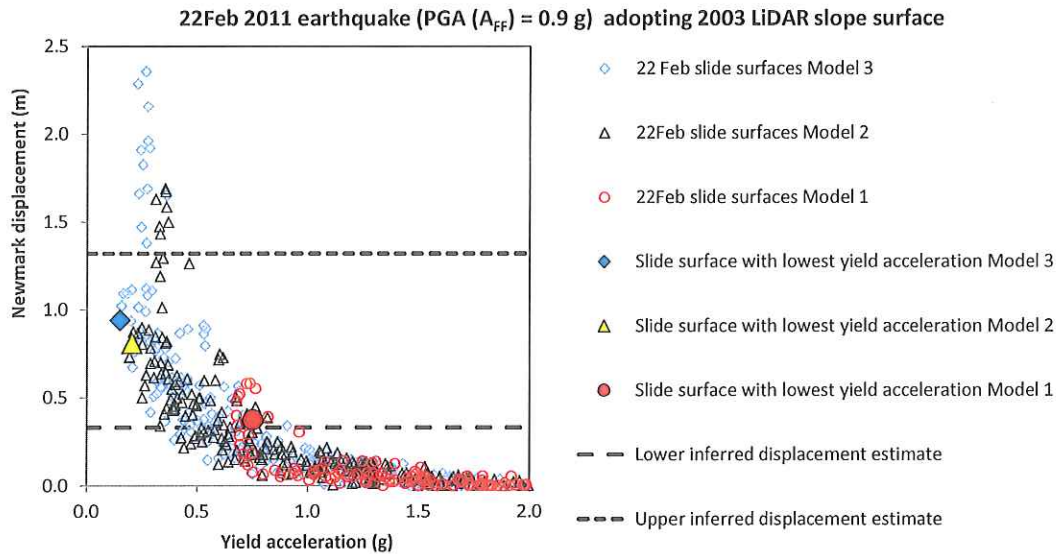
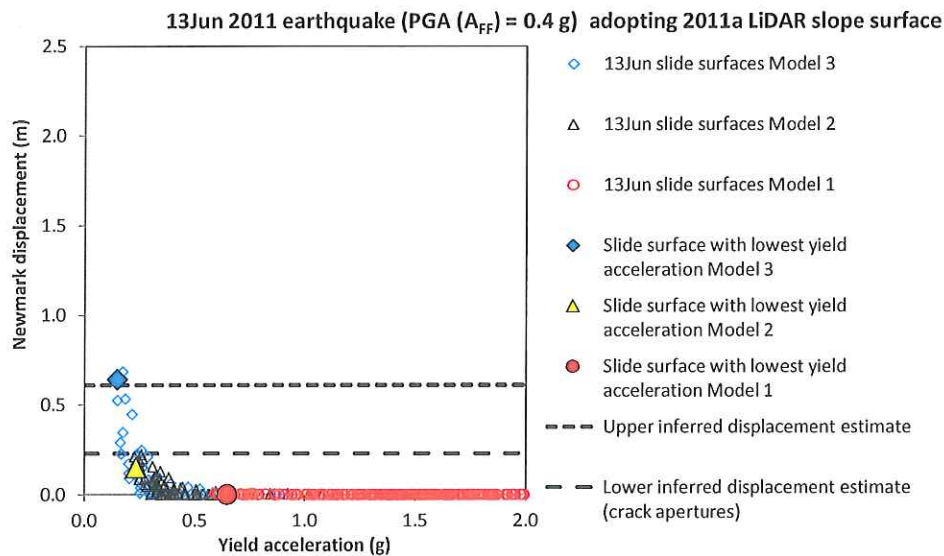


**Table 19** Results from the dynamic modelling of cross-section 4. Total inferred coseismic displacements are from measurements of crack apertures. Yield accelerations and permanent displacements are calculated from the decoupled assessment and represent the modelled slide surface with the lowest yield acceleration for the given material parameters and failure mechanism. Those rows highlighted in grey represent the material parameters that give the best correlation between the modelled and recorded permanent displacements, for a given earthquake and failure mechanism. Modelled displacements are rounded to the nearest 0.1 m.

Material parameter model (Table 17)	Earthquake	Lowest yield acceleration (g)	Min. modelled coseismic displacement (m)	Max. modelled coseismic displacement (m)	Total inferred coseismic displacement (m)
1	22 February 2011	0.68	0.5	0.6	0.3–1.3
1a	22 February 2011	0.29	0.7	1.1	0.3–1.3
2	22 February 2011	0.19	0.7	1.7	0.3–1.3
2a	22 February 2011	0	18.8	26.2	0.3–1.3
3	22 February 2011	0.15	0.9	2.4	0.3–1.3
1	13 June 2011	0.66	0.0	0.0	0.2–0.6
1a	13 June 2011	0.39	0.0	0.0	0.2–0.6
2	13 June 2011	0.23	0.2	0.2	0.2–0.6
2a	13 June 2011	0.01	2.1	2.4	0.2–0.6
3	13 June 2011	0.15	0.6	0.7	0.2–0.6



**Figure 23** Modelled Slope/W decoupled displacements of cross-section 4 for the 22 February 2011 earthquake and adopting variable estimates of the material strength. Each datapoint represents a modelled slide surface and the corresponding estimate of its displacement as a result of the 22 February 2011 earthquake – adopting the synthetic free-field rock outcrop earthquake acceleration time histories.  $A_{FF}$  is the peak horizontal ground acceleration of the free field motion used in the assessment. The dashed lines represent the total inferred coseismic permanent displacement of the slope along the cross-section during the given earthquake.



**Figure 24** 13 June 2011 earthquake, modelled Slope/W decoupled displacements for cross-section 4, and adopting variable estimates of the material strength. Each datapoint represents a modelled slide surface and the corresponding estimate of its displacement as a result of the 13 June 2011 earthquake – adopting the synthetic free-field rock outcrop earthquake acceleration time histories.  $A_{FF}$  is the peak horizontal ground acceleration of the free field motion used in the assessment. The dashed line represents the inferred coseismic permanent displacement of the slope along the cross-section during the given earthquake.

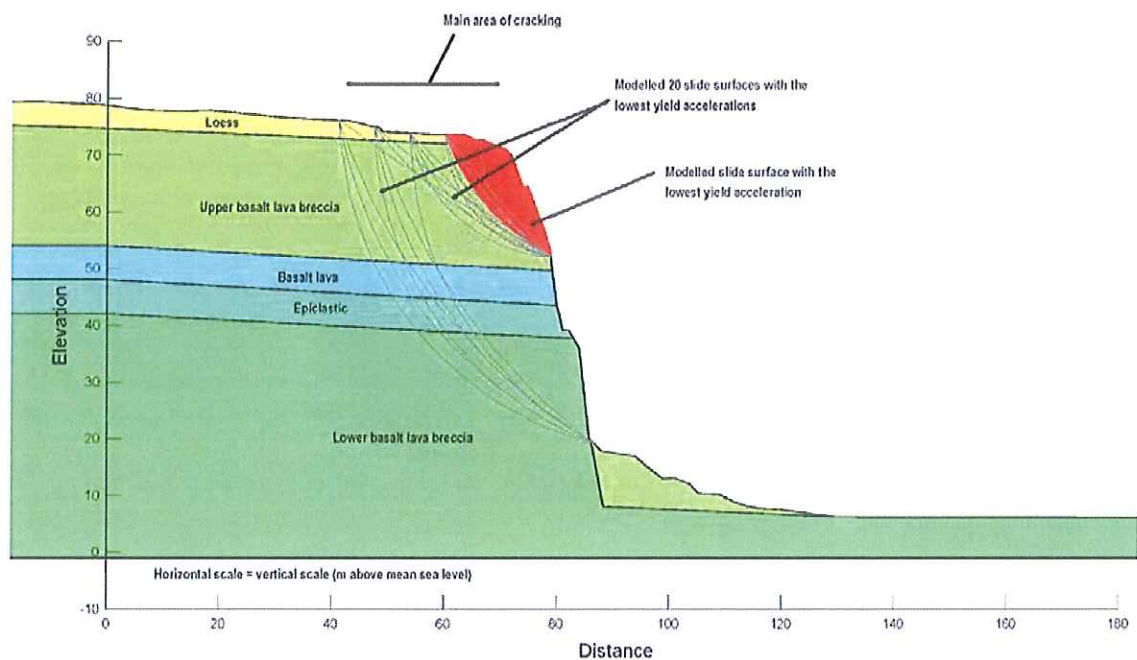


**Figure 25** Results from the seismic slope stability assessment for cross-section 4, for the 22 February 2011 earthquake, adopting model 1 material strength parameters.

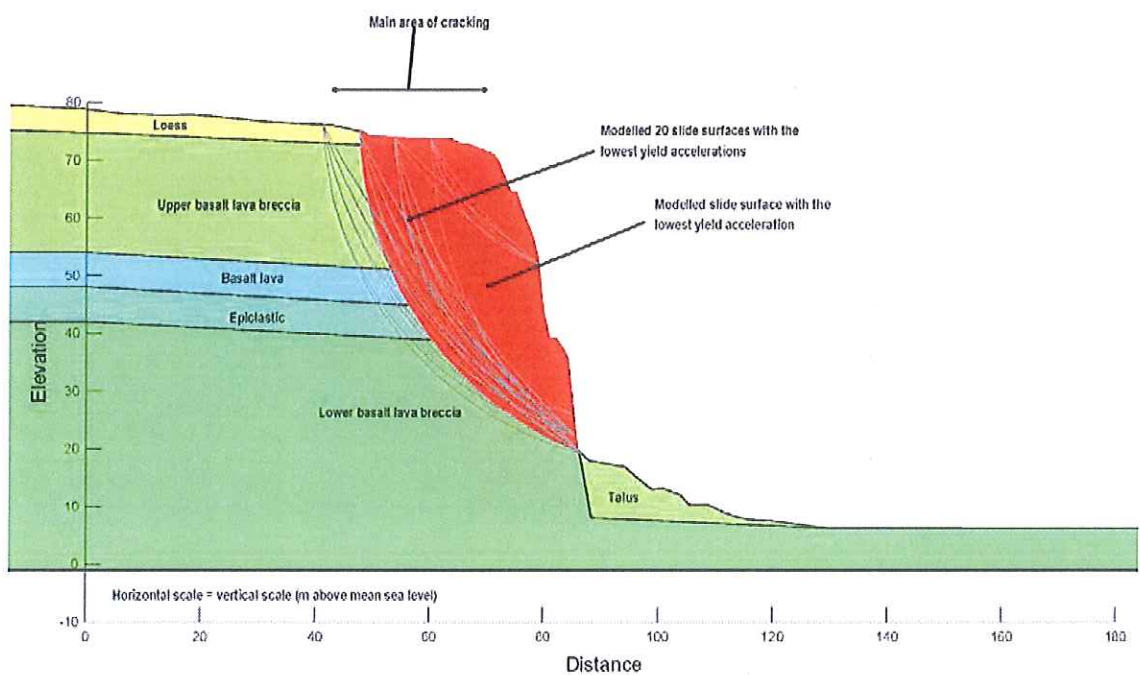


**Figure 26** Results from the seismic slope stability assessment for cross-section 4, for the 22 February 2011 earthquake, adopting model 2 material strength parameters.



The results show that:

- A good correlation between the inferred permanent coseismic displacements from crack apertures and modelled displacements of the slope for the 22 February 2011 earthquakes was obtained adopting material parameter models 1 and 2.
- A good correlation between the inferred permanent coseismic displacements from crack apertures and modelled displacements of the cliff for the 13 June 2011 earthquakes was obtained adopting material parameter models 2 and 3.
- The slide surfaces with the lowest yield accelerations adopting the upper range of material strength parameters (model 1) were mainly in the upper lava breccia, indicating a lower factor of safety of the upper part of the cliff.
- When the material strength parameters were degraded (i.e., adopting model 2 material strength parameters) the slide surfaces with the lowest yield accelerations are those that extend to the cliff toe, although the yield accelerations of the slide surfaces in the upper breccia are still low. These observations are consistent with the current slope condition, where recent cracks extend down from the crest to the toe.
- The slope material strength parameters may be reducing after each significant earthquake, as a result of the earthquake-induced fracturing and displacement of the rock mass.
- There is a good correlation between the locations and shape of the slide surfaces derived from the limit equilibrium and finite element static stability modelling, and those from the dynamic modelling.

#### 4.1.2.3 Forecast modelling of permanent slope deformation

Permanent displacements, from the decoupled assessment of results from the 22 February and 13 June 2011 modelled earthquakes, were calculated for a range of slide-surface geometries with different ratios of yield acceleration ( $K_y$ ) to the maximum average acceleration of the failure mass ( $K_{MAX}$ ) for a given slide surface. The maximum average acceleration ( $K_{MAX}$ ) was calculated for each selected slide surface by taking the maximum value of the average acceleration time history from the response to the synthetic earthquake. About 10-20 slide surfaces (with the lowest value of critical yield acceleration  $K_y$ ) were chosen to represent the results from each earthquake input motion, adopting different estimates of the shear strength of the main materials (models 2 and 3 in Table 17).

The results from the assessment are shown in Figure 27 for those slide surfaces shown in Figure 25 and Figure 26. The results show that between  $K_y/K_{MAX}$  values of 0.1 and 0.5, and  $K_y/A_{FF}$  values of 0.3 and 0.9, the data are well fitted to a straight line (exponential trend line) in semi-log space. The coefficient of determination ( $R^2$ ) is 0.89 for  $K_y/K_{MAX}$  and 0.82 for  $K_y/A_{FF}$ , and includes all of the plotted data ( $N = 79$ ). The lower coefficient of determination for ratios of  $K_y/A_{FF}$  is not unusual as Newmark (1965) displacements are highly sensitive to the high frequency components of the input motions, which can vary from event to event. By comparison,  $K_{MAX}$  "filters" the higher frequency components, and thus is less sensitive to the input motion characteristics.

The peak ground acceleration of the input motion ( $A_{FF}$ ) does not take into account amplification effects caused by the slope geometry (Appendix 5). From the data in Figure 27, the mean ratio of  $K_{MAX}$  to  $A_{FF}$  for cross-section 4 is 2.2 ( $\pm 0.3$  at one standard deviation), meaning that  $K_{MAX}$  is on average 2.2 times greater than the peak horizontal ground acceleration of the input motion, assuming a linear relationship.

For ratios of  $K_y/A_{MAX}$  in Figure 27, the estimated magnitudes of displacement are consistent with those reported by Jibson (2007), where these data plot between the ranges for earthquakes of M6.5–7.5 as reported by Makdisi and Seed (1978) and plotted by Jibson (2007).

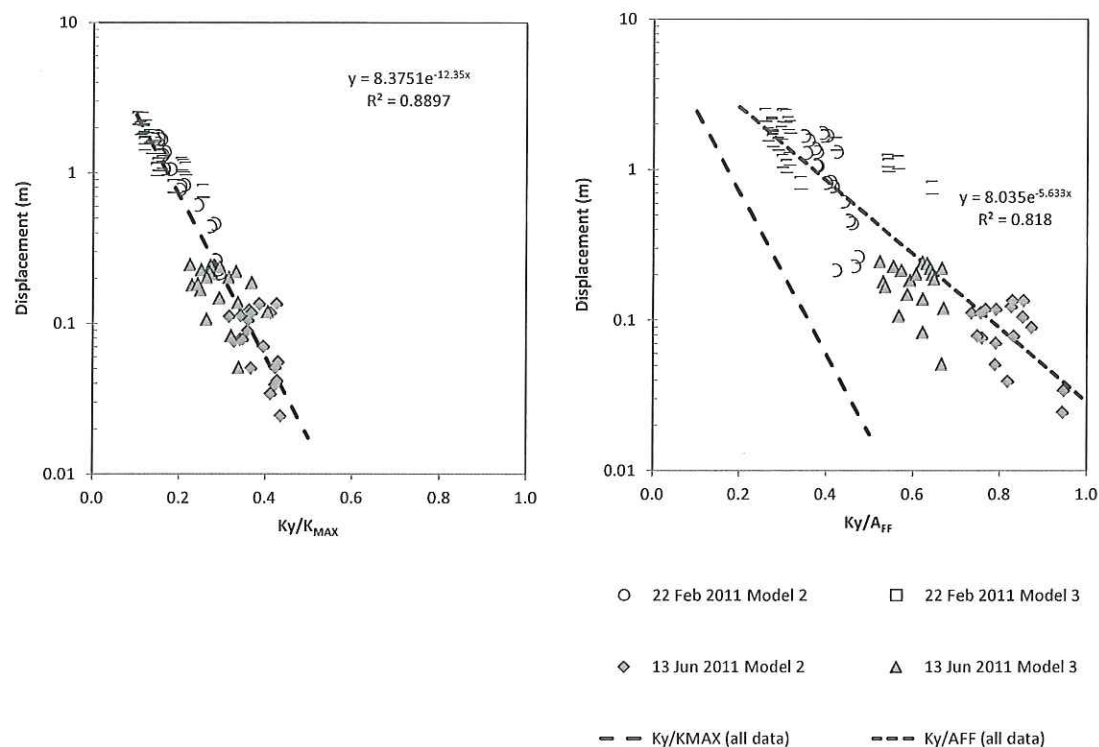


**Figure 27** Decoupled Slope/W displacements calculated for cross-section 4, for different ratios of yield acceleration to maximum average acceleration of the mass ( $K_y/K_{MAX}$ ), and maximum acceleration of the mass ( $K_y/A_{MAX}$ ), for selected slide-surface geometries, and given material shear strength parameter models 2 and 3.  $A_{MAX}$  is the peak acceleration of the input earthquake time acceleration history. Synthetic rock outcrop time acceleration histories for the 22 February and 13 June 2011 earthquakes were used as inputs for the assessment ( $N = 79$ ). The dashed lines are exponential trend lines fitted to the semi-log data. The formula and the coefficient of determination ( $R^2$ ) for the trend lines are shown.

The results from the decoupled assessment show that the magnitude of permanent slope displacement during an earthquake will vary in response to:

1. the shear strength of the rock mass at the time of the earthquake;
2. pore pressures within tension cracks and the rock mass, at the time of the earthquake; and
3. duration and amplitude of the earthquake shaking.

For cross-section 4, the relationship between the yield acceleration and the maximum average acceleration (from Figure 27) has been used to determine the likely range of displacements of a given failure mass with an adopted yield acceleration ( $K_y$ ) at given levels of peak free field horizontal ground accelerations ( $A_{FF}$ ) and the equivalent maximum average ground acceleration ( $K_{MAX}$ ). For cross-sections 2 and 6, the pseudostatic method of assessing the yield acceleration of each cross-section was used (the results are shown in Table 18), and the  $K_y/K_{MAX}$  relationship (Figure 27), established for cross-section 4, was used to determine the likely magnitude of permanent displacement in a future earthquake. This has been done using the seven earthquake event bands, used to represent the range of earthquake events the slopes could be subjected to in the future.

The results are shown in Table 20. Conservative yield accelerations have been adopted, assuming material parameter model 3, to take into account the possibility that the current shear strength of the materials is now degraded as a result of the past movement and cracking.

Displacement of the slide mass will not occur at maximum average accelerations ( $K_{MAX}$ ) less than the critical yield acceleration. However, the critical yield acceleration depends upon the strength of the slide surface at the time of the earthquake.

**Table 20** Forecast modelling results from the dynamic slope stability assessment for cross-sections 2, 4 and 6, adopting model 3 material parameters, and no water in tension cracks. Estimated displacements are rounded to the nearest 0.1 m.

Earthquake event band		1	2	3	4	5	6	7
Peak ground acceleration range of band (g)		0.1–0.3	0.3–0.5	0.5–0.8	0.8–1.2	1.2–1.6	1.6–2.0	2.0–3
Representative free field peak ground acceleration ( $A_{FF}$ ) for each band (g)		0.2	0.4	0.65	1.0	1.4	1.8	2.5
Adopted $K_{MAX}$ to $A_{FF}^1$ ratio		2.5 (mean plus 1 standard deviation)						
Cross-section	Adopted yield <sup>2</sup> acceleration ( $K_y$ ) (g)	Representative equivalent maximum average acceleration ( $K_{MAX}$ ) of each band (g)						
2	(0.3)	0.4	0.9	1.4	2.2	3.1	4.0	5.5
4	0.2	0.0	0.2	0.8	1.7	2.7	3.5	4.5
6	(0.5)	0.0	0.3	1.2	2.3	3.3	4.1	5.0
		0.0	0.0	0.1	0.6	1.2	1.9	2.9
		Estimated permanent displacement (m)						

<sup>1</sup>  $A_{FF}$  represents the peak horizontal ground acceleration of the free field input motion, rounded to the nearest 0.1 g.

<sup>2</sup> Where shown in brackets, the yield acceleration was calculated using the pseudostatic slope stability method.



#### 4.1.3 Slope stability – Summary of results

The main results from the static and dynamic stability assessment for assessed source areas 1–3 are:

1. Under current conditions, it is possible for failure of the trial slide surfaces to occur under either static or dynamic conditions. Material strengths – and therefore the slope factors of safety – may reduce with time (weathering), water content, and further movement of the slope under either static or dynamic conditions.
2. Under static and dynamic conditions the slide surfaces with the lowest factors of safety and those with the lowest yield accelerations ( $K_y$ ), are those associated with small failures at the crest and face of the slope, especially when water-filled tension cracks are included.
3. The most critical modelled slide surfaces are those with the lowest factors of safety and yield accelerations passing through the rock mass from slope crest to toe
4. Seismic site response assessment suggests that the peak ground amplification factors between the peak synthetic rock outcrop free-field accelerations and the modelled peak accelerations at the cliff crest vary between 2.6 for horizontal motions and up to 3.2 for vertical motions and that the relationship is non-linear.
5. Given the relatively low static factors of safety (1.4 and 1.1 for cross-sections 2 and 4 respectively), an increase in pore water pressures in open tension cracks within the overlying loess and joints within the underlying rock mass could lead to instability of the slope under static conditions (i.e., short duration high intensity rain).
6. Given the relatively low yield acceleration of the slope (estimated to be about 0.2 g for cross-section 4), it is likely that future earthquakes could reactivate the slope, leading to permanent displacements that could be quite large. The magnitude of any coseismic permanent displacements will depend upon:
  - a. The shear strength of the materials at the time of the earthquake;
  - b. The pore pressure/water content conditions within the slope at the time of the earthquake; and
  - c. The duration and amplitude of the earthquake shaking at the site.
7. Earthquake-induced failures are likely to be larger in volume and the debris travel further, than rainfall-induced failures.

It is inferred that parts of the cliff crest have already undergone more than one metre of permanent slope displacement during the 2010/11 Canterbury earthquakes. Given the thin layer of loess/fill above rock (1–2 m), the magnitude of displacement inferred from the sum of crack apertures suggest that failure/movement of the underlying rock has occurred. This displacement may have reduced the shear strength of critical materials in the slope, making the slope more susceptible to future earthquakes. In addition, there may be an unknown amount of further displacement that the slopes may be able to undergo before failing catastrophically (i.e., where the magnitude of displacement causes the failure mass to break down to become a mobile failure).